Electronic Supplementary Material (ESI) for RSC Advances.


**Supplementary Information:**

# Characterization and charge transfer properties of organic BODIPY dyes integrated in $TiO_2$ nanotubes based Dye-sensitized Solar Cells

I. Gonzalez-Valls,* A. Mirloup, T. Le Bahers, N. Keller, T. Cottineau,* P. Sautet, and V. Keller

## Optimization of the $TiO_2$ NTs synthesis by electrochemical anodization:

Several anodization parameters were studied for the formation of the $TiO_2$ NTs on the FTO slides, in Table S1 are reported all these conditions. The increase of the $NH_4F$ weight content from 0.3% to 0.5% promoted the anodization process (Figure S1a), the anodization time to consume the Ti layer and convert it in a transparent $TiO_2$ NTs layer was reduced by half. On the other hand, the increase of water volume content from 1 % to 3 %, slowed down the process but it also allowed the formation of a more homogeneous NT layer with a less drastic anodization method. As we can observe in Figure S1b, the current density final rise was earlier for 3% vol. $H_2O$. The most homogeneous anodization was obtained by using 0.5 % wt $NH_4F$ with 3 % vol. $H_2O$ in ethylene glycol (EG) electrolyte, applying a potential of 45 V and 18 °C temperature. However, in these conditions a thin layer of titanium was observed on top of the $TiO_2$ NTs after the anodization (Figure S2a). For this reason the temperature was increased from 18 °C to 30 °C to eliminate this titanium upper layer, but then the $TiO_2$ NTs appeared broken on the SEM images (Figure S2b). Thus, applying an intermediate temperature of 25 °C was found to be the optimum temperature to achieve the uniform layer of open-ended $TiO_2$ NTs. Figure S1c shows the temperature effect on the anodization speed process for 3 electrodes with the same thickness of sputtered Ti layer. Additionally, two different anodization potentials were applied to form the $TiO_2$ NTs, 45 V and 35 V. The potential is a very important parameter in the anodization technique; the applied voltage modifies the electric field between the electrolyte and the oxide layer, thus modifying the NTs diameter due to a faster or slower migration of the $F^-$ ions from the electrolyte into the $TiO_2$ layer. Increasing the voltage enhances both the growth rate formation of $TiO_2$ NTs and also the dissolution speed of the NTs with the complexation of $F^-$ producing $[TiF_6]^{2-}$ and as a result, it expands the NT diameters [1–4]. The 45 V potential was observed to give better results than the 35 V, the anodization was faster and more uniform.

**Table S1.** Electrochemical anodization conditions studied to optimize the preparation of $TiO_2$ NTs on FTO slides.

| $\%_{w/w}$ $NH_4F$ | $\%_{v/v}$ $H_2O$ | Temperature | Voltage |
|---|---|---|---|
| 0.3% | 1%<br>2% | 18 °C | 45 V |
| 0.5% | 1%<br>2%<br>3% | | |
| 0.3%<br>0.5% | 1%<br>3% | 30 °C | |
| **0.5%** | **3%** | **24 °C** | **45 V** |
| | | | 35 V |

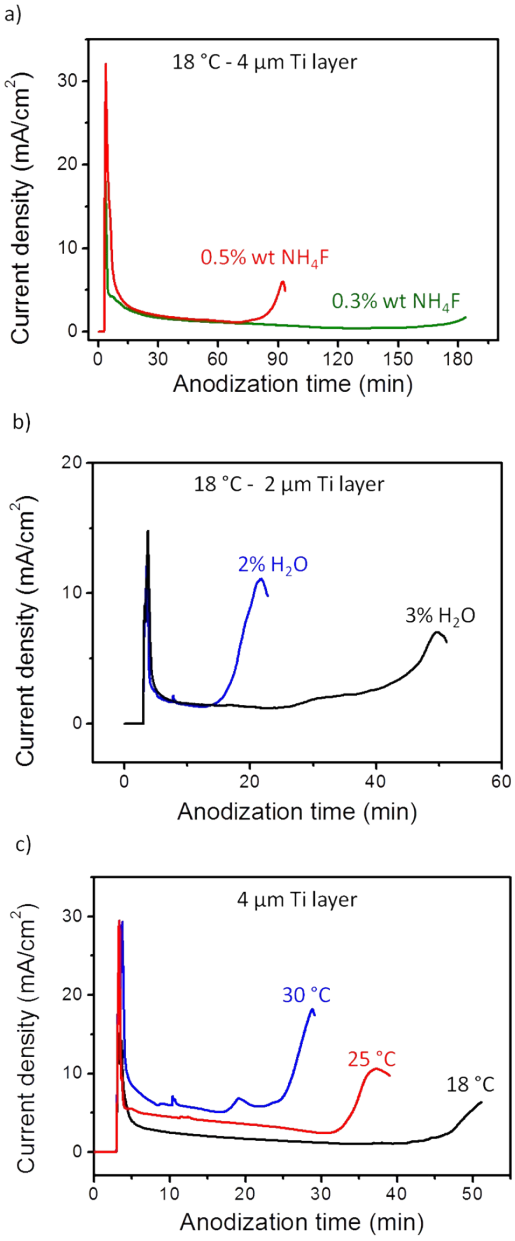


**Figure S1.** Effect of different conditions in the anodization process of the $TiO_2$ NTs preparation: a) $NH_4F$ content ($2\%_{v/v}$ $H_2O$ in EG, 18 °C, 45 V), b) $H_2O$ content (0.5%w/w $NH_4F$ in EG at 18°C, 45 V) and c) temperature ($3\%_{v/v}$ $H_2O$, $0.5\%_{w/w}$ $NH_4F$ in EG, 45 V).

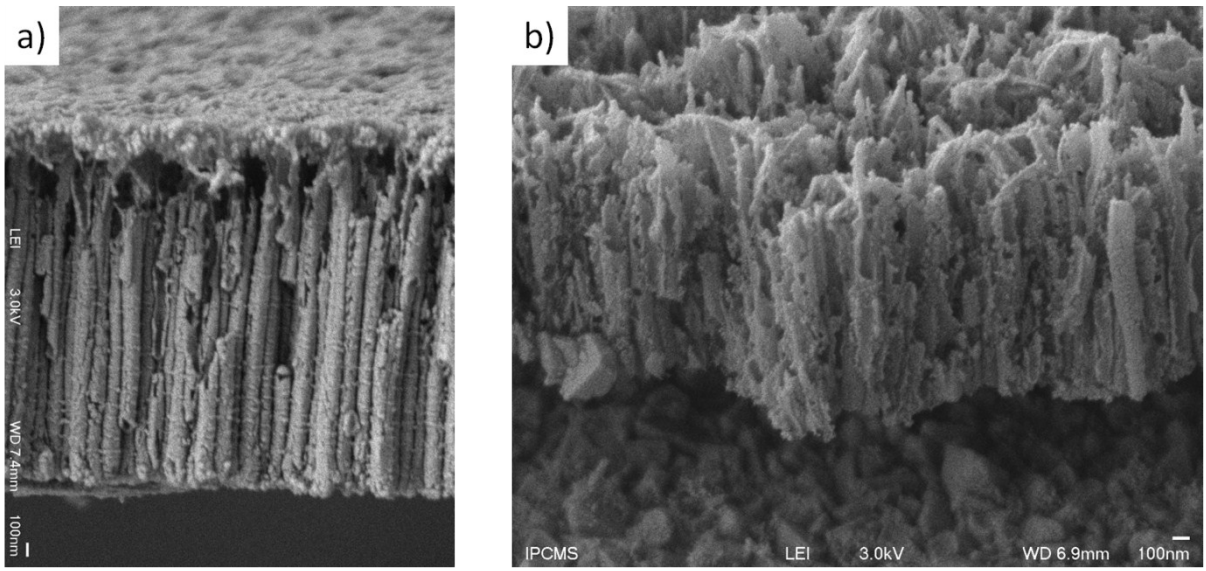


**Figure S2.** Cross-section SEM images tilted at 45° of electrode A prepared at different electrochemical anodization temperatures: a) 18 °C and b) 30 °C. The other anodization parameters were maintained the same: 0.5 % wt $NH_4F$ with 3 % vol. $H_2O$ in EG at 45 V.

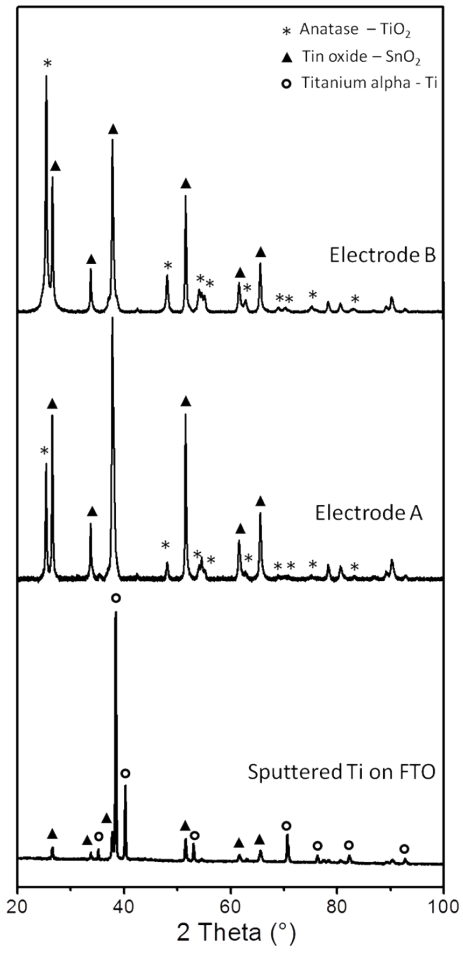


**Figure S3.** XRD analyses of $TiO_2$ NTs of electrode A and B and sputtered Ti on FTO.

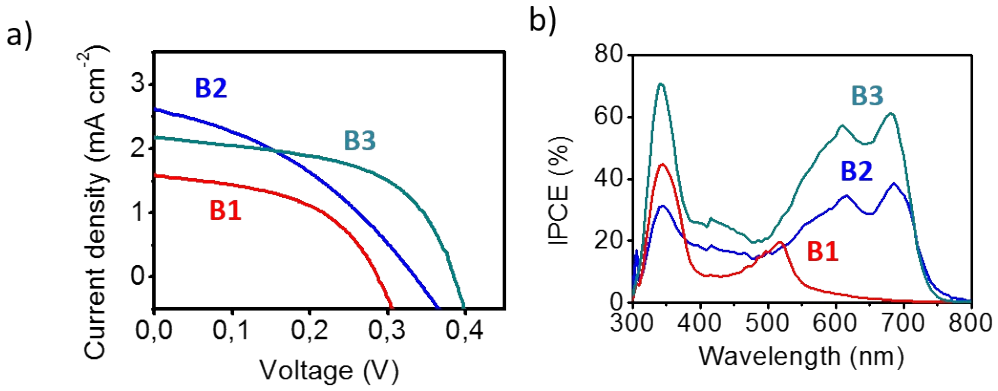


**Figure S4.** a) Current-voltage graphs of DSCs with electrode of 8.8 µm $TiO_2$ NTs length on titanium foil grafted with B1, B2 and B3 dyes and b) IPCE graphs of the same cells.

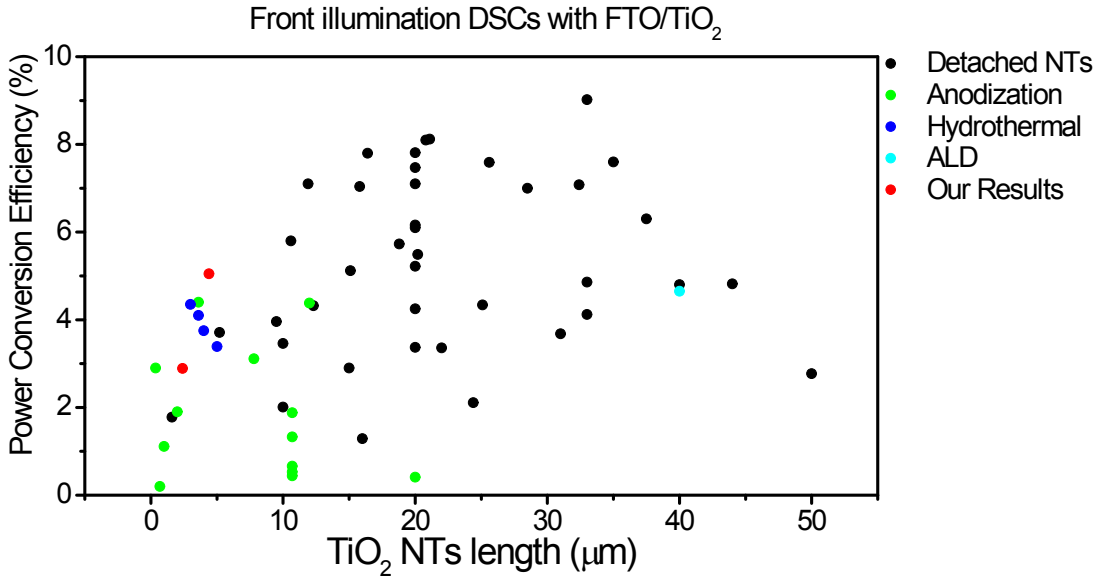


**Figure S5.** Power conversion efficiency vs.$TiO_2$ NTs length of reported DSCs with Ruthenium dyes (N719 or N3 dyes) from references [3,5–30], the results reported in this manuscript are in red.

**Table S2.** Photovoltaic and IPCE parameters for the DSCs obtained with electrode of 8.8 µm $TiO_2$ NTs length grown from titanium foil and grafted with B1, B2 and B3 dyes. Quantity of dye adsorbed measured by dye desorption.

| Dye | $V_{OC}$ (V) | $J_{SC}$ (mA·cm$^{-2}$) | FF (%) | PCE (%) | Dye adsorbed on the $TiO_2$ NTs ($10^{-8}$ mol·cm$^{-2}$) | IPCE (at $\lambda_{max}$) (%) |
|---|---|---|---|---|---|---|
| B1 | 0.29 | 1.57 | 49 | 0.22 | 3.6 | 20 % (515 nm) |
| B2 | 0.34 | 2.61 | 37 | 0.33 | 0.6 | 38 % (685 nm) |

| | | | | | | |
|---|---|---|---|---|---|---|
| B3 | 0.39 | 2.19 | 55 | 0.47 | 1.0 | 61 % (680 nm) |

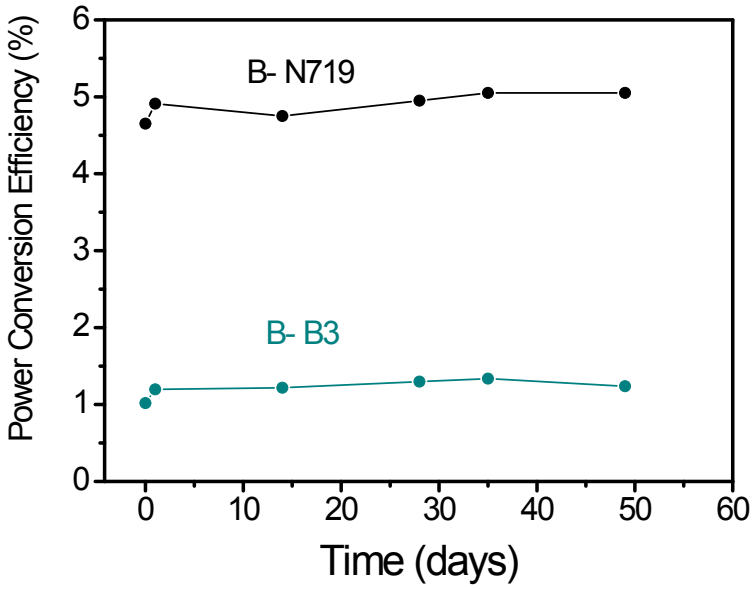


**Figure S6.** Power Conversion Efficiency with time of DSCs with 4.4 µm $TiO_2$ NTs length (electrode B) and N719 dye or B3 dye.

**Table S3.** Fitted results of EIS on DSCs with electrode A and B applying the dye N719 and B3. Electron lifetime (τ) measured from the frequency peak of Bode representation.

| Electrode | | | Voltage | $R_1$ | $C_2$ | $a_2$ | $R_2$ | $C_3$ | $a_3$ | $R_3$ | τ |
|---|---|---|---|---|---|---|---|---|---|---|---|
| | NT length (µm) | Dye | (V) | (Ω) | (F) | | (Ω) | (F) | | (Ω) | (ms) |
| A | 2.4 | N719 | 0.6 - dark | 108 | $5.4\ 10^{-7}$ | 0.80 | 15 | $1.4\ 10^{-4}$ | 0.87 | 327 | 22 |
| | | | 0.6 - light | 107 | $5.3\ 10^{-7}$ | 0.80 | 13 | $1.3\ 10^{-4}$ | 0.86 | 130 | 12 |
| B | 4.4 | N719 | 0.6 - dark | 95 | $1.0\ 10^{-6}$ | 0.80 | 15 | $4.2\ 10^{-4}$ | 0.83 | 144 | 38 |
| | | | 0.6 - light | 94 | $1.3\ 10^{-6}$ | 0.80 | 15 | $3.4\ 10^{-4}$ | 0.81 | 83 | 23 |
| A | 2.4 | B3 | 0.4 - dark | 68 | $1.5\ 10^{-6}$ | 0.80 | 11 | $2.2\ 10^{-4}$ | 0.92 | 2409 | 96 |
| | | | 0.4 - light | 67 | $1.8\ 10^{-6}$ | 0.80 | 8 | $2.2\ 10^{-4}$ | 0.93 | 590 | 38 |
| B | 4.4 | B3 | 0.4 - dark | 76 | $1.1\ 10^{-6}$ | 0.80 | 21 | $2.8\ 10^{-4}$ | 0.91 | 257 | 45 |
| | | | 0.4 - light | 75 | $9.1\ 10^{-7}$ | 0.80 | 20 | $2.7\ 10^{-4}$ | 0.90 | 131 | 23 |

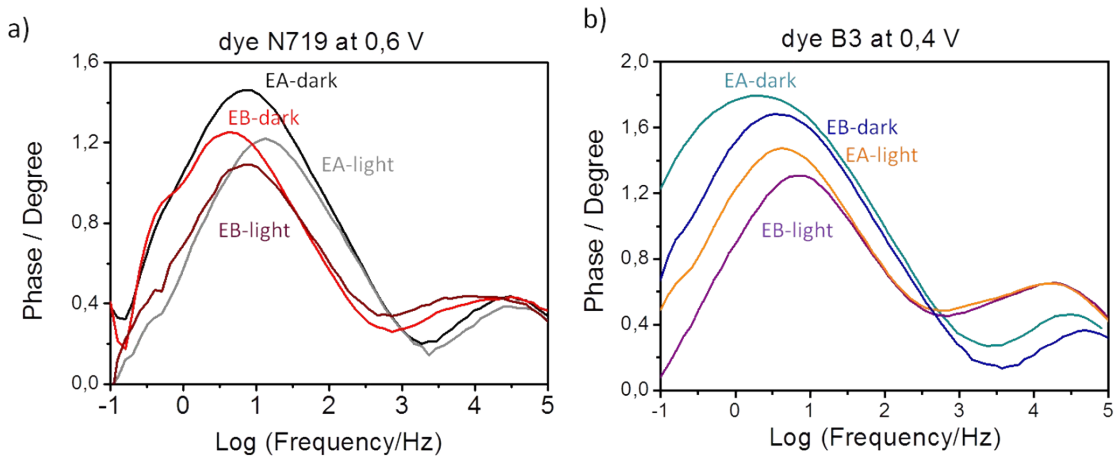


**Figure S7.** Bode plots of the EIS measurements for a) dye N719 based DSCs at 0.6 V and b) dye B3 based DSCs at 0.4 V.

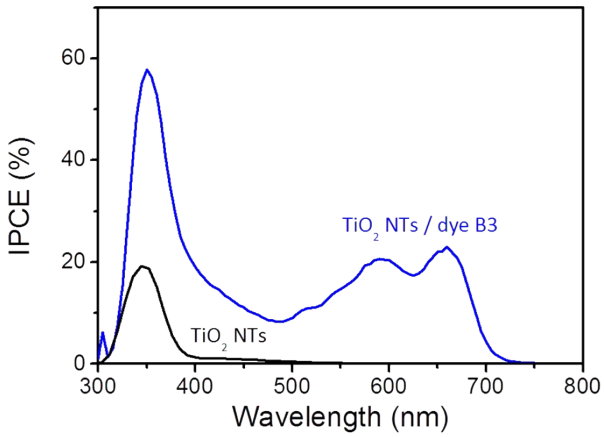


**Figure S8.** IPCE peaks of DSCs with electrode B without dye (black line) and with dye B3 (blue line).

## References


[1] G.K. Mor, O.K. Varghese, M. Paulose, C. a. Grimes, Adv. Funct. Mater. 15 (2005) 1291–1296.

[2] J. Wang, H. Wang, H. Li, J. Wu, Thin Solid Films 544 (2013) 276–280.

[3] Q. Pang, L. Leng, L. Zhao, L. Zhou, C. Liang, Y. Lan, Mater. Chem. Phys. 125 (2011) 612–616.

[4] S. Agarwala, G.W. Ho, J. Solid State Chem. 189 (2012) 101–107.

[5] X. Feng, K. Shankar, O.K. Varghese, M. Paulose, T.J. Latempa, C.A. Grimes, T. Pennsyl, V. State, V. Uni, U. V Park, V. Pennsyl, Nano Lett. 8 (2008) 3781–3786.

[6] J.H. Park, T.-W. Lee, M.G. Kang, Chem. Commun. (Camb). (2008) 2867–2869.

[7] X. Gao, D. Guan, J. Huo, J. Chen, C. Yuan, Nanoscale 5 (2013) 10438–46.

[8] A. Lamberti, A. Sacco, S. Bianco, D. Manfredi, M. Armandi, M. Quaglio, E. Tresso, C.F. Pirri, Sol. Energy 95 (2013) 90–98.

[9] S.H. Lee, S.Y. Chae, Y.J. Hwang, K.-K. Koo, O.-S. Joo, Appl. Phys. a-Materials Sci. Process. 112 (2013) 733–737.

[10] J. Lin, M. Guo, C.T. Yip, W. Lu, G. Zhang, X. Liu, L. Zhou, X. Chen, H. Huang, Adv. Funct. Mater. 23 (2013) 5952–5960.

[11] G.K. Mor, K. Shankar, M. Paulose, O.K. Varghese, C.A. Grimes, Nano Lett. 6 (2006) 215–218.

[12] Z. Yang, Z. Ma, D. Pan, D. Chen, F. Xu, S. Chen, Ceram. Int. 40 (2014) 173–180.

[13] J. Zhang, S. Li, H. Ding, Q. Li, B. Wang, X. Wang, H. Wang, J. Power Sources 247 (2014) 807–812.

[14] B. Lei, J. Liao, R. Zhang, J. Wang, C. Su, D. Kuang, (2010) 15228–15233.

[15] G. Ji, Z. Liu, D. Guan, Y. Yang, Appl. Surf. Sci. 282 (2013) 695–699.

[16] M. Paulose, K. Shankar, O.K. Varghese, G.K. Mor, C. a Grimes, J. Phys. D. Appl. Phys. 39 (2006) 2498–2503.

[17] Y. Liu, Y. Cheng, K. Chen, G. Yang, Z. Peng, Q. Bao, R. Wang, W. Chen, Electrochim. Acta 146 (2014) 838–844.

[18] W.-Y. Rho, H.-S. Kim, S.H. Lee, S. Jung, J.S. Suh, Y.-B. Hahn, B.-H. Jun, Chem. Phys. Lett. 614 (2014) 78–81.

[19] J. Choi, Y.S. Kwon, T. Park, J. Mater. Chem. A 2 (2014) 14380–14385.

[20] X. Liu, J. Lin, Y.H. Tsang, X. Chen, P. Hing, H. Huang, J. Alloys Compd. 607 (2014) 50–53.

[21] S. Sadhu, P. Poddar, J. Phys. Chem. C 118 (2014) 19363–19373.

[22] C.-H. Chen, K.-C. Chen, J.-L. He, Curr. Appl. Phys. 10 (2010) S176–S179.

[23] K.Y. Chun, B.W. Park, Y.M. Sung, D.J. Kwak, Y.T. Hyun, M.W. Park, Thin Solid Films 517 (2009) 4196–4198.

[24] X. Feng, K. Shankar, M. Paulose, C. a Grimes, Angew. Chem. Int. Ed. Engl. 48 (2009) 8095–8.

[25] Y. Ji, M. Zhang, J. Cui, K.-C. Lin, H. Zheng, J.-J. Zhu, A.C.S. Samia, Nano Energy 1 (2012) 796–804.

[26] S. Kathirvel, C. Su, C.-Y. Yang, Y.-J. Shiao, B.-R. Chen, W.-R. Li, Vacuum (2015) 1–9.

[27] H. Park, W.-R. Kim, H.-T. Jeong, J.-J. Lee, H.-G. Kim, W.-Y. Choi, Sol. Energy Mater. Sol. Cells 95 (2011) 184–189.

[28] H. Wang, H. Li, J. Wang, J. Wu, Mater. Lett. 80 (2012) 99–102.

[29] D.-J. Yang, H. Park, S.-J. Cho, H.-G. Kim, W.-Y. Choi, J. Phys. Chem. Solids 69 (2008) 1272–1275.

[30] W. Yuanhao, L. Lin, Y. Hongxing, Energy Procedia 61 (2014) 2608–2612.